

Solution Properties of Polymacromonomers Consisting of Polystyrene. 3. Viscosity Behavior in Cyclohexane and Toluene

Ken Terao, Toshio Hokajo, Yo Nakamura,* and Takashi Norisuye

Department of Macromolecular Science, Osaka University, Machikaneyama-cho 1-1, Toyonaka, Osaka 560-0043, Japan

Received January 21, 1999; Revised Manuscript Received March 31, 1999

ABSTRACT: Viscosity measurements have been made on two series of polymacromonomer samples consisting only of polystyrene (PS) and having fixed side chain lengths of 15 and 33 styrene residues (designated F15 and F33) in cyclohexane at 34.5 °C (the Θ temperature) and in toluene at 15 °C (a good solvent). The intrinsic viscosities $[\eta]$ obtained as functions of (total) weight-average molecular weight M_w (in the ranges from 5.1×10^3 to 6.5×10^6 for the F15 polymer and from 5.4×10^4 to 1.1×10^7 for the F33 polymer) are analyzed on the basis of the wormlike chain with or without excluded volume. They are described quantitatively by the current theories over the almost entire range of M_w studied, when the contribution of side chains near the main-chain ends to the polymacromonomer contour is incorporated into the analysis. The estimated parameters are consistent with those derived previously from gyration radius data, confirming that while the contour length per main-chain residue in the Θ or good solvent is close to the value expected for the *all-trans* conformation, the chain stiffness is much higher in the good solvent than in the Θ solvent due to enhanced monomer–monomer repulsions. The hydrodynamic diameter for each polymacromonomer in cyclohexane, slightly smaller than that in toluene, is about twice as large as the unperturbed end-to-end distance expected for the linear PS molecule having the same degree of polymerization as the side chain.

Introduction

In parts 1 and 2 of this series,^{1,2} we studied cyclohexane and toluene solutions of two series of polymacromonomer samples consisting only of polystyrene (PS) and having fixed side chain lengths of 15 and 33 styrene residues (polymacromonomers F15 and F33) by light scattering, and drew the following conclusions. 1. The two polymacromonomers have solubility features similar to those of linear PS in that they have a Θ point of 34.5 °C in cyclohexane and positive, large second virial coefficients in toluene at 15 °C; in the latter solvent, excluded-volume effects on $\langle S^2 \rangle_z$ (the z -average mean-square radius of gyration) are appreciable at high (total) molecular weights. 2. The main-chain length dependence of $\langle S^2 \rangle_z$ for the polymacromonomers in the two solvents is described quantitatively by the known theories^{3–6} for wormlike chains⁷ (or more generally, helical wormlike chains⁴) with or without excluded volume. 3. The chain stiffness expressed in terms of the Kuhn segment length λ^{-1} is an increasing function of side chain length and is higher in the good solvent (toluene) by about 1.6 times than in cyclohexane at the Θ point.

The present paper reports a viscometric study undertaken to see whether intrinsic viscosities $[\eta]$ for samples of the polymacromonomers F15 and F33 in the two solvents are consistent with the above conclusions from light scattering. In this connection, the following remarks are in order.

Wintermantel et al.^{8,9} and Nemoto et al.,¹⁰ analyzing dimensional and hydrodynamic data for polymacromonomers consisting of the poly(methyl methacrylate) (PMMA) backbone and PS side chains in toluene (a good solvent) on the basis of the unperturbed wormlike chain,⁷ found that λ^{-1} increases with side chain length. The work of the former group⁸ showed, however, that the available theories for this model did not give a consistent explanation of the measured $\langle S^2 \rangle_z$ and $[\eta]$. If literally taken, this finding indicates need of a new model for explaining

dilute-solution behavior of semiflexible polymacromonomers. We thus took interest in checking the applicability of the wormlike chain model to $[\eta]$ of our polymacromonomers or in finding a way to explain our $\langle S^2 \rangle_z$ and $[\eta]$ data consistently.

Experimental Section

Samples. The previously investigated samples^{1,2} (F15-1, F15-2, ..., F15-15 of the F15 polymer and F33-1, F33-2, ..., F33-10, F33-13, and F33-14 of the F33 polymer) with known weight-average molecular weights M_w were used for the present study (see Figure 1 in part 1 or part 2 for the chemical structure of the polymers). Most of these samples were previously investigated for molecular weight distribution by gel permeation chromatography in chloroform at 40 °C using the calibration curves constructed with the known M_w 's for the two series of polymacromonomer samples. The weight-average to number-average molecular weight ratios M_w/M_n determined were in the range between 1.05 and 1.12. The side chain length distribution was also examined for the precursor (α -benzyl- ω -hydrogen polystyrene) by a MALDI–TOF spectrometer and found to be characterized by M_w/M_n of 1.09 for F15 and 1.03 for F33. The molecular weights of the macromonomers were 3.56×10^3 for F33 and 1.65×10^3 for F15.^{1,2}

Viscometry. Viscosity measurements in cyclohexane at 34.5 °C and in toluene at 15 °C were made using a four-bulb low-shear capillary viscometer of the Ubbelohde type for samples F15-1, F15-2, F33-1, and F33-2 in toluene and conventional capillary viscometers for the rest; shear-rate effects on $[\eta]$ were small (less than 1%) when the $[\eta]$ values for the four samples from the two types of viscometer were compared. The two highest molecular weight samples of the F33 polymer (F33-1 and F33-2) in cyclohexane were not studied because they did not completely dissolve in the solvent at polymer mass concentrations c higher than 4×10^{-3} g cm⁻³ desirable for our viscometry. We note that the lowest c required was 20 times higher than the highest c studied by light scattering¹ since $[\eta]$ in cyclohexane at 34.5 °C was small even for high M_w (see Table 2).

In all measurements, the flow time was determined to a precision of 0.1 s with the difference between the solvent and

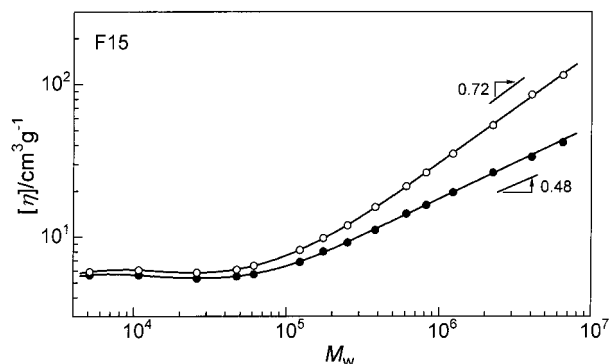


Figure 1. Molecular weight dependence of $[\eta]$ for the polymacromonomer F15 in cyclohexane at 34.5 °C (filled circles) and in toluene at 15 °C (unfilled circles).

Table 1. Results from Viscosity Measurements on Polymacromonomer F15 Samples in Cyclohexane at 34.5 °C and in Toluene at 15 °C

sample	$M_w/10^5$ ^a	in cyclohexane at 34.5 °C		in toluene at 15 °C	
		$[\eta]/\text{cm}^3 \text{g}^{-1}$	K'	$[\eta]/\text{cm}^3 \text{g}^{-1}$	K'
F15-1	64.7	41.6	0.71	115	0.36
F15-2	40.4	33.5	0.70	85.7	0.35
F15-3	22.5	26.4	0.75	53.9	0.39
F15-4	12.3	19.6	0.78	35.1	0.41
F15-5	8.22	16.2	0.87	26.4	0.46
F15-6	6.09	14.2	0.88	21.5	0.48
F15-7	3.81	11.1	0.95	15.7	0.55
F15-8	2.52	9.19	1.07	11.9	0.61
F15-9	1.75	8.02	1.09	9.81	0.66
F15-10	1.23	6.84	1.17	8.20	0.73
F15-11	0.614	5.68	1.18	6.46	0.86
F15-12	0.474	5.51	1.15	6.09	0.87
F15-13	0.260	5.33	1.13	5.82	0.85
F15-14	0.108	5.60	0.98	6.05	0.77
F15-15	0.0514	5.61	0.82	5.89	0.68

^a From light scattering in toluene.²

Table 2. Results from Viscosity Measurements on Polymacromonomer F33 Samples in Cyclohexane at 34.5 °C and in Toluene at 15 °C

sample	$M_w/10^5$ ^a	in cyclohexane at 34.5 °C		in toluene at 15 °C	
		$[\eta]/\text{cm}^3 \text{g}^{-1}$	K'	$[\eta]/\text{cm}^3 \text{g}^{-1}$	K'
F33-1	108			119	0.35
F33-2	76.5			91.4	0.35
D33-3	51.7	35.8	0.67	68.1	0.36
F33-4	36.2	28.5	0.71	51.6	0.38
F33-5	28.9	24.8	0.73	42.1	0.40
F33-6	22.0	21.4	0.75	33.5	0.43
F33-7	12.0	15.1	0.83	21.4	0.50
F33-8	8.73	11.5	0.88	17.3	0.53
F33-9	7.90	11.5	0.85	15.5	0.64
F33-10	3.84	8.20	1.04	10.2	0.75
F33-13	1.28	6.75	1.13	8.50	0.75
F33-14	0.543	6.95	1.09	8.66	0.78

^a From light scattering in toluene.²

solution flow times kept larger than 15 s. The relative viscosity was evaluated by taking account of the difference between the solution and solvent densities. The Huggins plot, the Fuoss–Mead plot, and the Billmeyer plot were combined to determine $[\eta]$ and the Huggins constant K' . The densities of solutions were measured with a pycnometer of the Lipkin–Davison type.

Results and Discussion

Molecular Weight Dependence of $[\eta]$. The values of $[\eta]$ and K' obtained are all summarized in Tables 1 and 2, along with those of M_w determined by light scattering in part 2.² The molecular weight dependence of $[\eta]$ for the polymacromonomer F15 in cyclohexane at

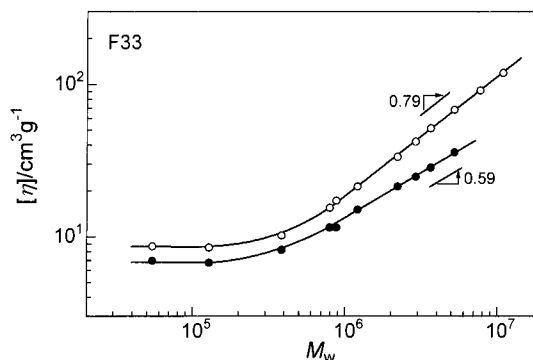


Figure 2. Molecular weight dependence of $[\eta]$ for the polymacromonomer F33 in cyclohexane at 34.5 °C (filled circles) and in toluene at 15 °C (unfilled circles).

Θ (34.5 °C) and in toluene at 15 °C is illustrated in Figure 1. The data points for the respective solvents are fitted by smooth curves which are almost horizontal up to a molecular weight of 6×10^4 and rise linearly with increasing M_w above 4×10^5 . The viscosity exponent in this high M_w region is 0.48 for cyclohexane solutions and 0.72 for toluene solutions.

The viscosity data for the polymacromonomer F33 in the two solvents, displayed in Figure 2, show similar main-chain length dependence, but the slopes of the curves in the high M_w region, i.e., for $M_w > 8 \times 10^5$, are larger than those for the F15 polymer in the corresponding solvents, being 0.59 in cyclohexane and 0.79 in toluene. The change in slope from 0 to 0.79 for toluene solutions is similar to what was reported for polymacromonomers consisting of the PMMA backbone and PS side chains in the same solvent at 25 °C.^{9,11}

Analysis. 1. Data in Cyclohexane at the Θ Point.

The intrinsic viscosity $[\eta]_0$ of an unperturbed wormlike chain was formulated by Yamakawa and co-workers^{12–14} with the cylinder and touched-bead models. For a given molecular weight M , it is determined by three parameters, the contour length L , the Kuhn segment length λ^{-1} , and the cylinder diameter d or the bead diameter d_b depending on the hydrodynamic model used for the calculation, and the theories based on the two models are essentially equivalent for thin, stiff chains ($\lambda d \leq 0.1$) if the difference between d and d_b are taken into account.¹⁴

For polymacromonomers, the cylinder model^{12,13} is probably suitable rather than the touched-bead model,¹⁴ but theoretical $[\eta]_0$ values for short, thick chains with flexibility are available only for the latter model because of the nature of the Kernel in the Kirkwood–Riseman type integral equation.^{12–14} Limited theoretical information on the cylinder model (capped with hemispheres at both ends) indicates, however, that the cylinder and touched-bead theories reduce to the Einstein equation for rigid spheres at $L = d = d_b$ and are identical if $L \gg d$ and d_b . Furthermore, the difference in $[\eta]_0$ between these theories with $d = d_b$ diminishes with increasing λd and becomes at most $\pm 5\%$ for $\lambda d = 0.2$ over the entire L range. Thus we may regard $[\eta]_0$ for the touched-bead chain model¹⁴ with $\lambda d_b \geq 0.2$ as that for the cylinder model and express the latter as

$$[\eta]_0 = f(\lambda L, \lambda d)/(\lambda^3 M) \quad (1)$$

where $f(\lambda L, \lambda d)$ is known as a function of λL and λd ($=\lambda d_b$); though $[\eta]_0$ in the touched-bead model is given only for the discrete number of beads, we regard that

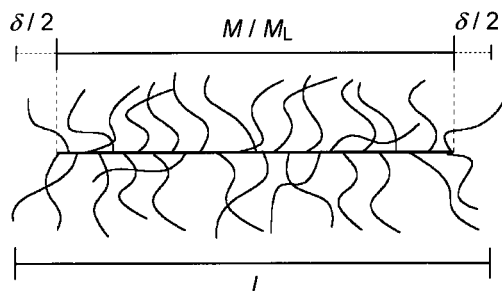


Figure 3. Schematic presentation of the effect of side chains on the contour length of a polymacromonomer.

Table 3. Wormlike Chain Parameters and Related Parameters for the Polymacromonomers F15 and F33 in Cyclohexane at 34.5 °C and in Toluene at 15 °C

polymer	solvent	$T/^\circ\text{C}$	$M_L/10^3 \text{ nm}^{-1}$	d/nm	δ/nm	λ^{-1}/nm	B/nm
F15	cyclohexane	34.5	6.3 (6.2) ^a	4.7	2.2	9.5 ^a	0
F15	toluene	15	6.3	5.0	2.3	16 ^a	4.5 ^a
F33	cyclohexane	34.5	13.5 (13.0) ^a	7.4	4.0	22 ^a	0
F33	toluene	15	13.8	8.5	4.3	36 ^a	18 ^a

^a Analysis from $\langle S^2 \rangle_z$ data.^{1,2}

in eq 1 as a continuous function of L . It should be noted that L is related to M by $L = M/M_L$, with M_L being the molar mass per unit contour length.

With the values of λ^{-1} (9.5 nm for F15 and 22 nm for F33)^{1,2} previously determined from $\langle S^2 \rangle_z$ in cyclohexane at 34.5 °C, we attempted to estimate a set of M_L and d which allows eq 1 to fit the $[\eta]$ data for F15 or F33 in cyclohexane. However, no parameter set explained the very gradual M_w dependence of $[\eta]$ in the low molecular weight region (see Figures 1 and 2).

As remarked in our previous work^{1,2} on $\langle S^2 \rangle_z$, some side chains near the main-chain ends may contribute toward apparently increasing L . This end effect is schematically shown in Figure 3, in which $\delta/2$ stands for the hydrodynamic contribution of side chains to the main-chain contour at each end. With this new parameter, L may be redefined by

$$L = M/M_L + \delta \quad (2)$$

In applying eq 1 with this equation, we ignore the difference between the segment density near each main-chain end and that in the middle portion of the polymer backbone, and assume that both ends of the polymacromonomer are hemispherical. We note that the end effect or side chain effects on $\langle S^2 \rangle$ were negligible in the molecular-weight range studied by light scattering in parts 1 and 2.^{1,2}

Again with the λ^{-1} values from $\langle S^2 \rangle_z$, the viscosity data in cyclohexane were analyzed by eq 1 with eq 2. The estimated parameters (M_L , d , and δ), together with the values of λ^{-1} and M_L from $\langle S^2 \rangle_z$ ^{1,2} are summarized in Table 3, and the theoretical $[\eta]_0$ values (the solid lines) are compared with our data in Figure 4, in which the left end of each solid curve corresponds to the Einstein sphere limit.¹⁵ The fits of the curves to the data points for the respective polymacromonomers are good down to this limit. The dot-dashed lines in the figure represent the theoretical values for $\delta = 0$. Their deviations from the solid lines become large progressively with decreasing molecular weight below 1×10^6 , showing pronounced end effects on $[\eta]$.

The values of M_L from $[\eta]$ and $\langle S^2 \rangle_z$ for the respective polymacromonomers in Table 3 agree well with each

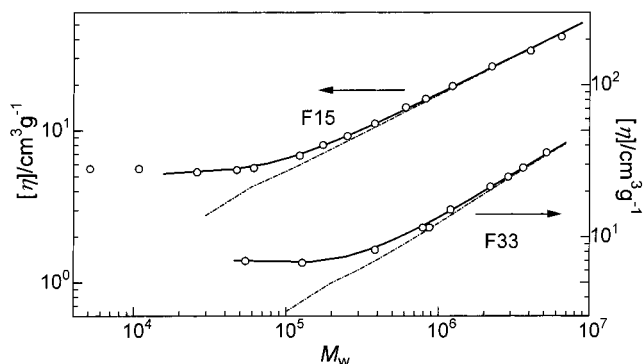


Figure 4. Comparison between the measured $[\eta]$ (circles) for the polymacromonomers F15 and F33 in cyclohexane at 34.5 °C and the theoretical solid curves calculated from eq 1 with eq 2 for the unperturbed wormlike chains with the parameters given in Table 3. Dot-dashed lines show theoretical values for $\delta = 0$.

other, implying that essentially the same wormlike-chain parameters (λ^{-1} and M_L) explain our $\langle S^2 \rangle_z$ and $[\eta]$ data in cyclohexane. These M_L 's with the molecular weights of the macromonomers (1.65×10^3 for F15 and 3.56×10^3 for F33)^{1,2} give the monomeric length (along the main-chain contour) values of about 0.26 nm, which are close to that (0.25 nm) calculated on the assumption that the backbone assumes the *all-trans* conformation. In short, the wormlike chain is a good model for the two polymacromonomers in cyclohexane at the Θ temperature.

As the λ^{-1} values in Table 3 indicate, the polymacromonomers in cyclohexane are considerably stiff, but the viscosity exponents (0.48 for F15 and 0.59 for F33) are unusually small even at high M_w where the end effect is negligible. According to the $[\eta]_0$ theory based on the cylinder^{12,13} or touched-bead¹⁴ model, the viscosity exponent is determined not by λ^{-1} itself but by the magnitude of λd and is smaller for larger λd . In fact, the λd values for our polymers F15 and F33 in cyclohexane are 0.49 and 0.33, respectively, being comparable to that for linear PS in the same solvent.¹⁶ Thus, these polymacromonomers in the Θ state exhibit viscosity behavior as if they were flexible.

2. Data in Toluene. As shown in parts 1 and 2,^{1,2} excluded volume effects on $\langle S^2 \rangle_z$ for the polymacromonomers F15 and F33 in toluene are appreciable at high M_w and explained quantitatively by the quasi-two-parameter (QTP) theory⁴⁻⁶ for wormlike⁷ or helical wormlike⁴ bead chains. Within the framework of this theory, the viscosity-radius expansion factor $\alpha_\eta \equiv ([\eta]/[\eta]_0)^{1/3}$ is a universal function of the scaled excluded-volume parameter \tilde{z} defined by

$$\tilde{z} = \frac{3}{4} K(\lambda L) z \quad (3)$$

with

$$z = \left(\frac{3}{2\pi} \right)^{3/2} (\lambda B) (\lambda L)^{1/2} \quad (4)$$

and

$$K(\lambda L) = \frac{4}{3} - 2.711(\lambda L)^{-1/2} + \frac{7}{6}(\lambda L)^{-1} \quad \text{for } \lambda L > 6$$

$$= (\lambda L)^{-1/2} \exp[-6.611(\lambda L)^{-1} + 0.9198 + 0.03516\lambda L] \quad \text{for } \lambda L \leq 6 \quad (5)$$

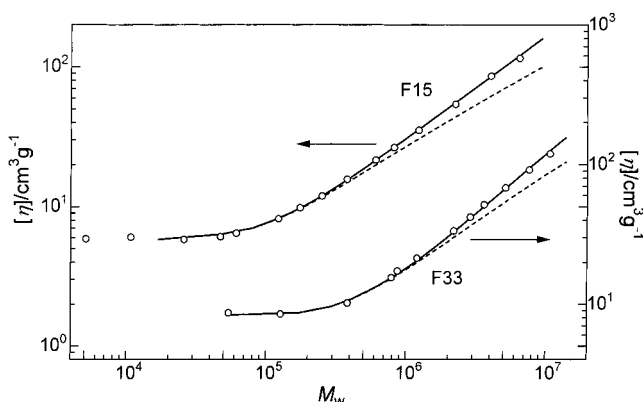


Figure 5. Comparison between the measured $[\eta]$ (circles) for the polymacromonomers F15 and F33 in toluene at 15 °C and the theoretical solid curves calculated from eqs 1 and 7 with eq 2 for the perturbed wormlike chains with the parameters given in Table 3. Dashed lines show theoretical values for the unperturbed intrinsic viscosity.

Here, z is the conventional excluded-volume parameter and B is the excluded-volume strength defined for the wormlike chain by

$$B = \beta/a^2 \quad (6)$$

with β and a being the binary cluster integral representing the interaction between a pair of beads and the bead spacing, respectively.

Adopting the Barrett function¹⁷ for α_η^3 , we have⁴

$$\alpha_\eta^3 = (1 + 3.8\tilde{z} + 1.9\tilde{z}^2)^{0.3} \quad (7)$$

which reduces to the original Barrett equation in the coil limit where $\tilde{z} = z$. Equation 7 is known to accurately describe experimental data for linear flexible^{18–21} and semiflexible polymers²² over a broad range of molecular weight.

Equations 1–7 indicate that five parameters, λ^{-1} , M_L , d , δ , and B , need to be known in order to evaluate $[\eta]$ in a perturbed state as a function of M . A curve fitting procedure was employed for our analysis with λ^{-1} and B fixed to the values determined previously² from $\langle S^2 \rangle_z$ data in toluene; we note that more than three parameters could not uniquely be determined from the present $[\eta]$ data. The estimated parameters of M_L , d , and δ are presented in Table 3, along with the assumed values for λ^{-1} and B . Figure 5 shows that the theoretical solid curves calculated with these parameters for the two polymacromonomers closely fit the data points down to the sphere limit. This agreement may be taken to substantiate that the wormlike chain model is applicable to our polymacromonomers in the good solvent, too, since the estimated M_L and hence the monomeric contour length for each polymer essentially agree with those from both $\langle S^2 \rangle_z$ and $[\eta]$ in cyclohexane at the Θ temperature. The dashed lines in Figure 5 refer to the unperturbed state (i.e., $B = 0$). Their downward deviations from the perturbed lines show the significance of excluded volume effects on $[\eta]$ for our polymacromonomers with high molecular weights in toluene. Though not shown here, the end effects on $[\eta]$ were remarkable at low M_w as in cyclohexane (see the dot-dashed lines in Figure 4). Hence, consideration of both excluded-volume and end effects seems almost mandatory in the analysis of $[\eta]$ data for a polymacromonomer covering

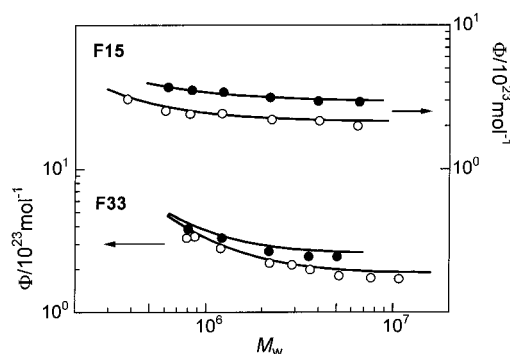


Figure 6. Experimental Φ values for the polymacromonomers F15 and F33 in cyclohexane at 34.5 °C (filled circles) and in toluene at 15 °C (unfilled circles) compared with the theoretical values (see the text for the parameters used).

a broad range of M_w in a good solvent, though the former effect in a stiffer chain is generally less significant.

Viscosity Factor. The circles, filled and unfilled, in Figure 6 show the values of the Flory viscosity factor $\Phi = [\eta]M_w/(6\langle S^2 \rangle_z)^{3/2}$ for our polymacromonomers in cyclohexane and toluene, respectively, calculated from the data in Tables 1 and 2 and the previous $\langle S^2 \rangle_z$ data.² As M_w increases, Φ gradually decreases, and for both polymers it is systematically larger in the Θ solvent than in the good solvent. These features resemble those for short flexible chains^{4,18,23} rather than long stiff chains.²⁴

The curves in Figure 6 represent the theoretical Φ values for the wormlike chains computed with the parameters in Table 3 from eqs 1–7 and the following expressions for the unperturbed mean-square radius of gyration³ $\langle S^2 \rangle_0$ and the radius expansion factor $\alpha_s (= \langle S^2 \rangle^{1/2}/\langle S^2 \rangle_0^{1/2})$ in the QTP scheme^{4–6} with the Domb–Barrett function:²⁵

$$\langle S^2 \rangle_0 = \frac{L}{6\lambda} - \frac{1}{4\lambda^2} + \frac{1}{4\lambda^3 L} - \frac{1}{8\lambda^4 L^2} [1 - \exp(-2\lambda L)] \quad (8)$$

$$\alpha_s^2 = \left[1 + 10\tilde{z} + \left(\frac{70\pi}{9} + \frac{10}{3} \right) \tilde{z}^2 + 8\pi^{3/2} \tilde{z}^3 \right]^{2/15} [0.933 + 0.067 \exp(-0.85\tilde{z} - 1.39\tilde{z}^2)] \quad (9)$$

We note that the means of M_L from $[\eta]$ and $\langle S^2 \rangle_z$ (6250 nm^{−1} for F15 and 13400 nm^{−1} for F33) have been used for the calculation and also that, as already mentioned, the end effect on $\langle S^2 \rangle_z$ can be neglected in the M_w range concerned here. Though the curves for F33 appear somewhat above the data points because of the small discrepancy between the M_L values from $\langle S^2 \rangle_z$ and $[\eta]$, the agreement between theory and experiment is rather satisfactory. This confirms that $\langle S^2 \rangle_z$ and $[\eta]$ for our polymacromonomers in both Θ and good solvents are consistently explained by the wormlike chain model.

Chain Diameter. As expected, the value of d for the polymacromonomer F33 in cyclohexane or toluene, given in Table 3, is considerably larger than that for F15, and both are much larger than what is known for linear PS in cyclohexane ($d = 0.75$ nm or $d_b = 1.01$ nm).^{4,16} We suspected that the hydrodynamic diameter for either polymacromonomer in cyclohexane at the Θ temperature is roughly twice as large as the unperturbed root-mean-square end-to-end distance $\langle R^2 \rangle_0^{1/2}$ of the linear PS chain with same number of monomer units as each side chain (the side chain molecular weight is $1.53 \times$

10^3 for F15 and 3.44×10^3 for F33),^{1,2} and calculated $\langle R^2 \rangle_0^{1/2}$ from the known expression⁴ for the unperturbed helical wormlike chain with $\lambda^{-1}\kappa_0$ (the reduced curvature) = 3.0, $\lambda^{-1}\tau_0$ (the reduced torsion) = 6.0, λ^{-1} (the static stiffness parameter) = 2.06 nm, and $M_L = 358 \text{ nm}^{-1}$.^{26,27} The resulting values of $\langle R^2 \rangle_0^{1/2}$ are 2.4 nm for F15 and 3.8 nm for F33, which are indeed in good agreement with the $d/2$ values for the polymacromonomers in cyclohexane (see Table 3).

The estimated diameters for both polymacromonomers in toluene at 15 °C are slightly larger than those in cyclohexane at 34.5 °C. The difference for the F33 polymer is more than the uncertainty in our estimation and thus indicates that enhancement of repulsion between neighboring side chains in toluene causes the side chains to extend. As found from $\langle S^2 \rangle_z$ in part 2² and confirmed indirectly from $[\eta]$ in this work, the chain stiffness also increases when the solvent is changed from the Θ to good solvent condition. Thus, intramolecular excluded-volume interactions between the main chain and side chains and between neighboring side chains play an important role in the global conformation or structure of a polymacromonomer in solution.

Conclusions

We obtained $[\eta]$ data covering a broad range of M_w for two polymacromonomer samples consisting of 15 (F15) and 33 (F33) styrene side chain residues in cyclohexane at 34.5 °C (a Θ solvent) and in toluene at 15 °C (a good solvent), and analyzed them on the basis of the Kratky–Porod wormlike chain. These data can be explained almost quantitatively by the current theories for this model with or without excluded volume when the end effect arising from side chains near the main-chain ends is considered. The estimated parameters are consistent with those determined previously from $\langle S^2 \rangle_z$, confirming the conclusion from light scattering that for the two polymacromonomers F15 and F33 the chain stiffness is higher in the good solvent than in the Θ solvent, while the monomeric length along the backbone contour is close to that expected for the *all-trans* conformation in both solvents. The hydrodynamic diameter for each polymer in cyclohexane is about twice as large as the unperturbed root-mean-square end-to-end distance of the linear polystyrene chain with the same number of monomer units as each side chain in the polymacromonomer. The diameter in toluene is slightly larger than that in cyclohexane, indicating that repulsions between neighboring side chains cause not

only the backbone stiffness but also the average side chain length to increase.

References and Notes

- (1) Terao, K.; Takeo, Y.; Tazaki, M.; Nakamura, Y.; Norisuye, T. *Polym. J.* **1999**, *31*, 193.
- (2) Terao, K.; Nakamura, Y.; Norisuye, T. *Macromolecules* **1999**, *32*, 711.
- (3) Benoit, H.; Doty, P. *J. Phys. Chem.* **1953**, *57*, 958.
- (4) Yamakawa, H. *Helical Wormlike Chains in Polymer Solutions*; Springer: Berlin, 1997.
- (5) Yamakawa, H.; Stockmayer, W. H. *J. Chem. Phys.* **1972**, *57*, 2843.
- (6) Shimada, J.; Yamakawa, H. *J. Chem. Phys.* **1986**, *85*, 591.
- (7) Kratky, O.; Porod, G. *Recl. Trav. Chim. Pays-Bas* **1949**, *68*, 1106.
- (8) Wintermantel, M.; Schmidt, M.; Tsukahara, Y.; Kajiwarra, K.; Kohjiya, S. *Macromol. Rapid Commun.* **1994**, *15*, 279.
- (9) Wintermantel, M.; Gerle, M.; Fischer, K.; Schmidt, M.; Wataoka, I.; Urakawa, H.; Kajiwarra, K.; Tsukahara, Y. *Macromolecules* **1996**, *29*, 978.
- (10) Nemoto, N.; Nagai, M.; Koike, A.; Okada, S. *Macromolecules* **1995**, *28*, 3854.
- (11) Tsukahara, Y.; Kohjiya, S.; Tsutsumi, K.; Okamoto, Y. *Macromolecules* **1994**, *27*, 1662.
- (12) Yamakawa, H.; Fujii, M. *Macromolecules* **1974**, *7*, 128.
- (13) Yamakawa, H.; Yoshizaki, T. *Macromolecules* **1980**, *13*, 633.
- (14) Yoshizaki, T.; Nitta, I.; Yamakawa, H. *Macromolecules* **1988**, *21*, 165.
- (15) The values of λd for the polymacromonomers in cyclohexane are not sufficiently small compared to unity, implying that the polymers are not completely rigid even in the sphere limit where $L = d$. However, the present analysis ignores such small flexibility of the two hemispherical caps at the chain ends. Though the values of δ themselves may have no much significance, they are about half those of d (see Table 3) and seem reasonable.
- (16) Einaga, Y.; Koyama, H.; Konishi, T.; Yamakawa, H. *Macromolecules* **1989**, *22*, 3419.
- (17) Barrett, A. J. *Macromolecules* **1984**, *17*, 1566.
- (18) Abe, F.; Einaga, Y.; Yamakawa, H. *Macromolecules* **1993**, *26*, 1891.
- (19) Horita, K.; Abe, F.; Einaga, Y.; Yamakawa, H. *Macromolecules* **1993**, *26*, 5067.
- (20) Abe, F.; Horita, K.; Einaga, Y.; Yamakawa, H. *Macromolecules* **1994**, *27*, 725.
- (21) Kamijo, M.; Abe, F.; Einaga, Y.; Yamakawa, H. *Macromolecules* **1995**, *28*, 1095.
- (22) Norisuye, T.; Tsuboi, A.; Teramoto, A. *Polym. J.* **1996**, *28*, 357.
- (23) Akashi, K.; Nakamura, Y.; Norisuye, T. *Polymer* **1998**, *39*, 5209.
- (24) See, for example, Murakami, H.; Norisuye, T.; Fujita, H. *Macromolecules* **1980**, *13*, 345.
- (25) Domb, C.; Barrett, A. J. *Polymer* **1976**, *17*, 179.
- (26) Konishi, T.; Yoshizaki, T.; Saito, T.; Einaga, Y.; Yamakawa, H. *Macromolecules* **1990**, *23*, 290.
- (27) Konishi, T.; Yoshizaki, T.; Yamakawa, H. *Macromolecules* **1991**, *24*, 5614.

MA990091O